International Journal of Mass Spectrometry 308 (2011) 275–280

Contents lists available at ScienceDirect

International Journal of Mass Spectrometry

journal homepage: www.elsevier.com/locate/ijms

Energetics and dynamics of dissociation of deprotonated peptides: Fragmentation of angiotensin analogs

Julia Laskin*, Zhibo Yang[1]

Pacific Northwest National Laboratory, Chemical and Materials Sciences Division, Richland, WA, USA

ARTICLE INFO

Article history:
Received 19 May 2011
Received in revised form 30 June 2011
Accepted 6 July 2011
Available online 30 July 2011

Keywords:
Surface-induced dissociation
Deprotonated peptide
Threshold energy
Activation entropy
Charge-remote fragmentation

ABSTRACT

We present a first study of the energetics and dynamics of dissociation of deprotonated peptides using time- and collision-energy resolved surface-induced dissociation (SID) experiments. SID of four model peptides (RVYIHPF, HVYIHPF, DRVYIHPF, and DHVYIHPF) was studied using a specially designed Fourier transform ion cyclotron resonance mass spectrometer (FT-ICR MS) configured for studying ion-surface collisions. Energy and entropy effects for the overall decomposition of the precursor ion were deduced by modeling the time- and collision energy-resolved survival curves using an RRKM based approach developed in our laboratory. The results were compared to the energetics and dynamics of dissociation of the corresponding protonated species. We demonstrate that acidic peptides are less stable in the negative mode because of the low threshold associated with the kinetically hindered loss of H_2O from $[M-H]^-$ ions. Comparison between the two basic peptides indicates that the lower stability of the $[M-H]^-$ ion of RVYIHPF as compared to HVYIHPF towards fragmentation is attributed to the differences in fragmentation mechanisms. Specifically, threshold energy associated with losses of NH_3 and NHCNH from RVYIHPF is lower than the barrier for backbone fragmentation that dominates gas-phase decomposition of HVYIHPF. The results provide a first quantitative comparison between the energetics and dynamics of dissociation of $[M+H]^+$ and $[M-H]^-$ ions of acidic and basic peptides.

1. Introduction

Tandem mass spectrometry (MS/MS) is widely used in applications focused on identification of peptides and proteins [1]. These studies examine structure-specific fragmentation of positive or negative ions of the analyte molecules in the gas-phase. Identification of the precursor ion relies on the basic understanding of the dissociation pathways. The distribution of product ions in MS/MS spectra is determined by the energetics and dynamics of dissociation of peptide ions, the internal energy distribution of the vibrationally excited ions, and the time frame of the experiment [2,3]. Soft ionization techniques such as electrospray (ESI) [4] or matrix assisted laser desorption ionization (MALDI) [5] are commonly used to generate both positive and negative ions of peptides and proteins for subsequent MS/MS characterization. Because of the higher ionization yields obtained in the positive mode, fragmentation of protonated peptides has been extensively investigated [6–13]. Gas-phase fragmentation of protonated peptides is commonly initiated by the transfer of the ionizing proton followed by heterolytic cleavage of the backbone bond [9]. Collision-induced dissociation (CID) of protonated peptides typically results in cleavages of the amide bonds and the formation of b- and y-ions [10]. These processes have been extensively studied using both experimental and theoretical approaches.

In contrast, relatively little is known about the energetics and mechanisms of fragmentation of deprotnated peptides. Bowie and co-workers conducted high-energy CID studies for a variety of deprotonated peptide sequences [14]. Losses of small neutral molecules (e.g., NH_3, H_2O, CO_2, NHCNH) often dominate dissociation of small di- and tripeptides [15] while larger ions undergo facile amide and N–C_α bond cleavages. Many fragmentation pathways are catalyzed by the charged groups. For example, Beauchamp and co-workers demonstrated that the loss of the deprotonated C-terminal amino acid resulting in formation of the y_1 ion may be catalyzed by the deprotonated C-terminal carboxyl group [16]. Similarly, acidic residues often promote backbone fragmentation of the deprotonated peptides. For example, Brinkworth et al. [17] showed that CID spectra of deprotonated peptides containing aspartic (D) and glutamic acid (E) residues are dominated by selective cleavages of N–C_α bonds at the acidic residues, which could be used to identify the presence and position of D and E in the sequence. Similar

* Corresponding author at: Pacific Northwest National Laboratory, P.O. Box 999 K8-88, Richland, WA 99352, USA. Tel.: +1 509 371 6136; fax: +1 509 371 6139.
E-mail address: Julia.Laskin@pnnl.gov (J. Laskin).
[1] Current address: Department of Chemistry and Biochemistry, University of Colorado, Boulder, CO, USA.

1387-3806/$ – see front matter © 2011 Elsevier B.V. All rights reserved.
doi:10.1016/j.ijms.2011.07.003

selective fragmentation was reported by Harrison [18] who demonstrated that N–C_α bond cleavages occur directly from $[M-H]^-$ precursor ions when D is positioned at the C-terminus. However, loss of H_2O precedes N–C_α bond fragmentation when D is located inside the sequence.

Although selective N–C_α bond cleavages at acidic residues result in formation of c- and z-ions, CID spectra of deprotonated acidic peptides are dominated by b- and y-ions produced through non-selective amide bond cleavages [19,20]. In contrast, c-ions are often dominant backbone fragments of basic peptides [21,22]. Cassady and co-workers compared post-source decay (PSD) of $[M+H]^+$ and $[M-H]^-$ ions of several basic peptides. They observed y-ion formation in both positive and negative modes [21]. In addition, abundant c-ions and minor a-ions were observed in the negative mode. The c-ion formation was particularly pronounced for peptides lacking acidic residues suggesting that the observed N–C_α bond cleavage likely involves a mobile deprotonation site along the peptide backbone or charge-remote fragmentation. More recently the same group examined fragmentation of polyalanine peptides containing one basic residue [22]. This study demonstrated that basic residues have little or no effect on the dissociation of deprotonated peptides. Efficient hydrogen atom scrambling in CID of deprotonated peptides reported by Bache et al. [23] indicates that amide hydrogens undergo facile migration prior to fragmentation of vibrationally excited deprotonated peptides. It follows that migration of amide hydrogens is likely responsible for the N–C_α bond cleavages observed in the negative mode CID of basic peptides. However, the presence of acidic residues may promote other low-energy dissociation pathways suppressing the efficiency of c-ion formation [15].

In this study we examined the effect of the acidic and basic residues on the stability of deprotonated peptides using time- and collision-energy resolved surface-induced dissociation (SID) experiments on a specially designed Fourier transform ion cyclotron resonance mass spectrometer (FT-ICR MS) [24]. We used two acidic and two basic angiotensin analogs as model systems. The energetics, dynamics and mechanisms of fragmentation of protonated angiotensin ions have been studied in great detail [25,26], which make these ions ideal candidates for obtaining detailed understanding of the effect of the charge and sequence on the stability of gaseous peptide ions. Time- and collision-energy resolved SID combined with Rice–Ramsperger–Kassel–Marcus (RRKM) modeling of the experimental data is a valuable tool for studying the energetics and dynamics of the gas-phase fragmentation of peptide ions and non-covalent complexes [11,27,28]. Here we report the first study focused of the energetics and dynamics of dissociation of deprotonated peptides.

2. Experimental

2.1. Chemicals

Angiotensin II and III (DRVYIHPF and RVYIHPF) and 1-dodecanethiol were purchased from Sigma/Aldrich (St. Louis, MO). DHVYIHPF and HVYIHPF were synthesized according to literature procedures. Fmoc-protected amino acids and the Wang resin were purchased from Advanced ChemTech (Louisville, KY). Samples were dissolved in a 70:30 (v/v) methanol:water solution containing 1% acetic acid to a final concentration of ca. 50 μM. A syringe pump (Cole Parmer, Vernon Hills, IL) was used for direct infusion of the electrospray samples at flow rates ranging from 20 to 50 μL/h.

2.2. SID target

The self-assembled monolayer surface of 1-dodecanethiol (HSAM) was prepared on a single gold {1 1 1} crystal (Monocrystals, Richmond Heights, OH) using a standard procedure. The target was cleaned in a UV cleaner (Model 135500, Boekel Industries Inc., Feasterville, PA) for 10 min and allowed to stand in a solution of 1-dodecanethiol for 10 h. The target was removed from the SAM solution and washed ultrasonically in ethanol for 10 min to eliminate extra layers.

2.3. Surface-induced dissociation experiments

SID experiments were conducted on a specially fabricated 6 T FTICR mass spectrometer described in detail elsewhere [24]. The SID target is introduced through a vacuum interlock assembly and positioned at the rear trapping plate of the ICR cell. Ions are electrosprayed at atmospheric pressure and transferred into the vacuum system via an electrodynamic ion funnel and a collisional quadrupole. Mass selection is achieved using an Extrel quadrupole (mass range up to 4000 amu) controlled by a 300 W, 880 kHz 150-QC Extrel power supply (Extrel, Pittsburgh, PA). Mass-selected ions are accumulated for 0.2–1 s in a collisional octopole held at $(2–5)\times10^{-3}$ Torr and transferred into the ICR cell. SID experiments are performed by allowing ions collide with the surface positioned at the rear trapping plate of the ICR cell. The collision energy is defined by the difference between the potential applied to the accumulation quadrupole and the potential applied to the rear trapping plate and the SID target. In the negative mode, scattered ions are captured by decreasing the potentials on the front and rear trapping plates of the ICR cell by 10–20 V. Time-resolved mass spectra were acquired by varying the delay between the gated trapping and the excitation/detection event (the reaction delay) from 1 ms to 1 s. Immediately following the fragmentation delay, ions are excited through a broadband chirp and detected.

2.4. RRKM modeling

Time-dependent survival curves (SCs) were constructed from experimental mass spectra by plotting the relative abundance of the corresponding ion as a function of collision energy for each delay time. SCs were modeled using an RRKM-based approach described elsewhere [29,30]. First, the microcanonical rate coefficient, $k(E)$, was calculated as a function of internal energy using the microcanonical RRKM/QET expression. Next, the survival probability of the precursor ion as a function of the internal energy of the ion and the experimental observation time was calculated from the rate-energy $k(E)$ dependency, taking into account radiative decay of the excited ion population. The overall signal intensity at a given collision energy was obtained by integrating the survival probability over the internal energy distribution of vibrationally excited ions. The internal energy deposition function was determined by fitting the experimental SCs of the singly protonated RVYIHPF, for which the dissociation parameters are known from our previous studies [25].

Vibrational frequencies of the peptide were adopted from our previous study [25]. Vibrational frequencies for the transition state were estimated by removing one C–N stretch (reaction coordinate) from the parent ion frequencies, as well as scaling all frequencies in the range of 500–1000 cm^{-1} to obtain the best fit with experimental data. The calculated SCs were compared to the experimental data. The fitting parameters included critical energies and activation entropies for different dissociation channels of the precursor ion. They were varied until the best fit to experimental SCs was obtained.

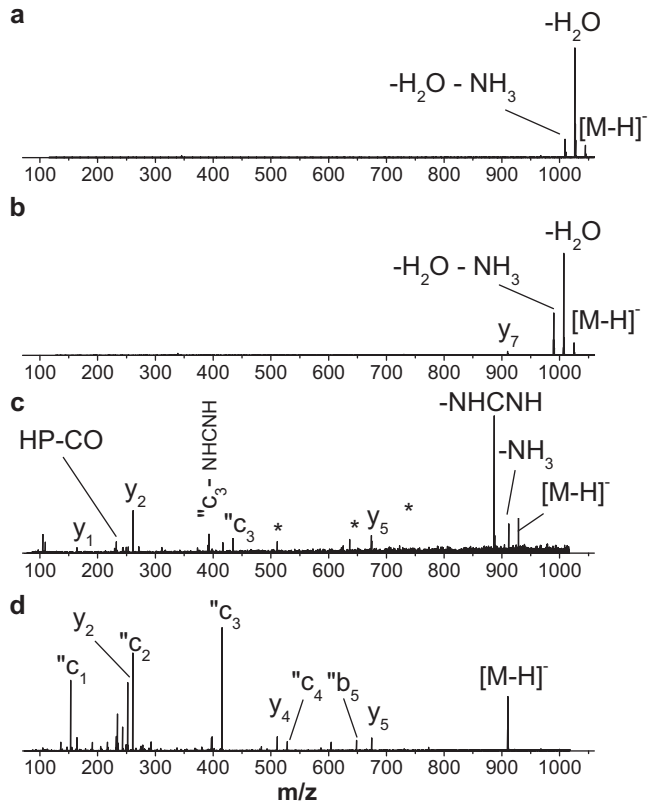

Fig. 1. Surface-induced dissociation spectra corresponding to ca. 90% fragmentation of (a) DRVYIHPF at 48.5 eV; (b) DHVYIHPF at 53.5 eV; (c) RVYIHPF at 87.5 eV; (d) HVYIHPF at 98.5 eV for 1 s reaction delay.

3. Results and discussion

3.1. Fragmentation pathways

In this study we used acidic and basic angiotensin analogs (DRVYIHPF, DHVYIHPF, RVYIHPF and HVYIHPF) to examine the energetics and dynamics of dissociation of deprotonated peptides in the gas-phase. Fig. 1 shows SID spectra of these species corresponding to ca. 90% fragmentation of the precursor ion at 1 s reaction delay; all SID fragments are listed in Table 1. Note that we adopted the fragment nomenclature used by Harrison [31], in which backbone cleavages are indicated using standard symbols (a, b, c, x, y, z) and primes refer to the number of lost or added hydrogens. For example, in this nomenclature y_n^- refers to the negative y-ion two mass units less than the positive $y_n''^+$ product ion while $''c_n^-$ corresponds to a negative c-ion two mass units less than the positive c_n^+ product ion. Dissociation of acidic peptides is dominated by the loss of water molecule followed by sequential losses of H_2O, NH_3, CO_2, and NHCNH [17]. Backbone fragments are observed as minor products at high collision energies. SID of both DRVYIHPF and DHVYIHPF results in formation of a complete series of y-ions. In addition, N-terminal backbone fragmentation is observed for DHVYIHPF following H_2O and NH_3 losses.

Fragmentation of deprotonated RVYIHPF (Fig. 1c) is initiated by the loss of NHCNH from the arginine side chain [17]. Collision energy resolved data shown in Fig. 2a indicate that primary low-energy dissociation channels for this precursor ion correspond to losses of NHCNH and NH_3 while higher appearance energies are associated with the formation of backbone fragments. In contrast, backbone fragments are primary dissociation products of the deprotonated HVYIHPF (Figs. 1d and 2b). SID of basic peptides produces a number of abundant c- and y-type backbone fragments. In addition, an even-electron $'''z_1$ ion and several b- and a-ions were observed for HVYIHPF. These observations are consistent with the previous study by Cassady and co-workers who examined fragmentation of deprotonated polyalanine peptides containing basic residues [22].

3.2. Relative stabilities of $[M-H]^-$ and $[M+H]^+$ ions

Relative stabilities of the four peptides towards fragmentation are compared in Fig. 3. The presence of an acidic residue in the sequence has a strong destabilizing effect on peptide anions resulting in more than 30 eV shift in the position of SCs between acidic and basic peptides. The relative stability towards fragmentation increases in the order DRVYIHPF < DHVYIHPF < <RVYIHPF < HVYIHPF. Fig. 4 compares the experimentally measured collision energies required to observe 50% fragmentation of the precursor ion ($E_{50\%}$) for $[M+H]^+$ and $[M-H]^-$ ions of the four angiotensin analogs examined in this study for reaction delay times of 1 ms and 1 s. The value of $E_{50\%}$ is determined by the amount of the internal energy required to observe fragmentation (the kinetic shift), the reaction delay and the efficiency of the kinetic-to-internal (T–V) transfer in collisions. Because the T–V transfer efficiency is the same for all ions compared in Fig. 4, the differences in the $E_{50\%}$ values are attributed to the differences in the kinetic shifts [32]. The kinetic shift is strongly dependent on the threshold energy for dissociation (E_0) and the activation entropy

Table 1
Fragment ions observed for $[M-H]^-$ precursor ions of acidic and basic angiotensin analogs. Major fragments are highlighted in bold.

	DRVYIHPF	*DHVYIHPF*
Acidic peptides		
Common fragments	**M-H_2O**, **M-H_2O–NH_3**, M-2H_2O–NH_3, M-NH_3–H_2O–CO_2, y_7, y_6, **y_5**, y_4, y_2	
Distinct fragment	**M-2NH_3–H_2O**, M-H_2O–NHCNH, M-NH_3–H_2O–NHCNH, $''x_6$, $''$H	M-3H_2O–NH_3, $''b_6$–H_2O–NH_3, $''a_6$-2H_2O–NH_3, $''a_5$-2H_2O–NH_3, $''b_4$–H_2O, $''$IH, y_1
	RVYIHPF	*HVYIHPF*
Basic peptides		
Common fragments	**y_5**, **y_4**, $''$**c_3**, $''$**b_3**, $''$**c_2**, **y_2**, $''$**c_2**-H_2O, $''$IH, **y_2-NH_3**, **y_2-H_2O**, y_1	
Distinct fragments	**M-NH_3**, **M-NHCNH**, $''$**c_3-NHCNH**, $'''$**c_3-NHCNH**	$''b_5$, $''b_5$–CO_2, $''$HP, $''a_2$-H_2O, $C_7H_6N_3O_2$ (His), $C_7H_{11}N_2O_2$ (Ile), $''$**c_1**, $'''z_1$

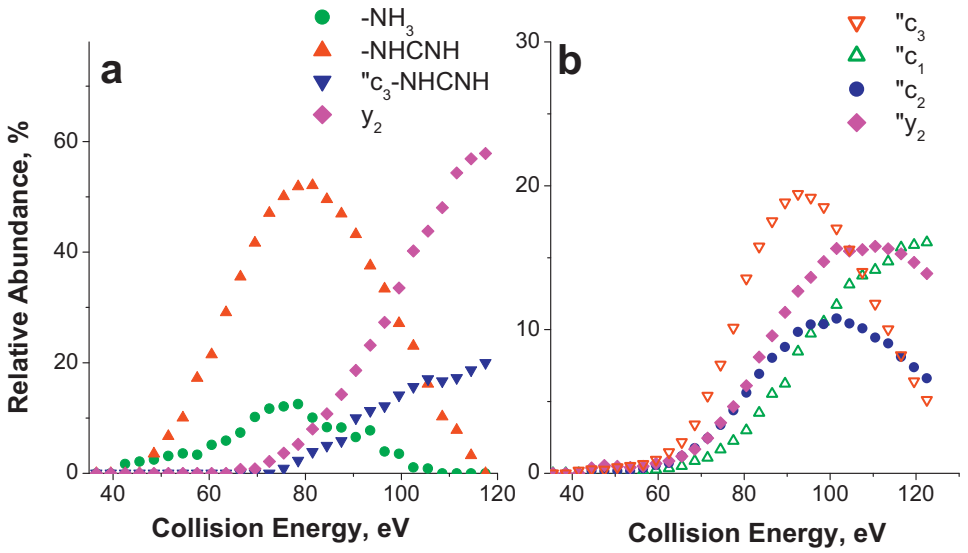

Fig. 2. Fragmentation efficiency curves obtained for major fragments of the deprotonated (a) RVYIHPF; (b) HVYIHPF at a reaction delay of 1 s.

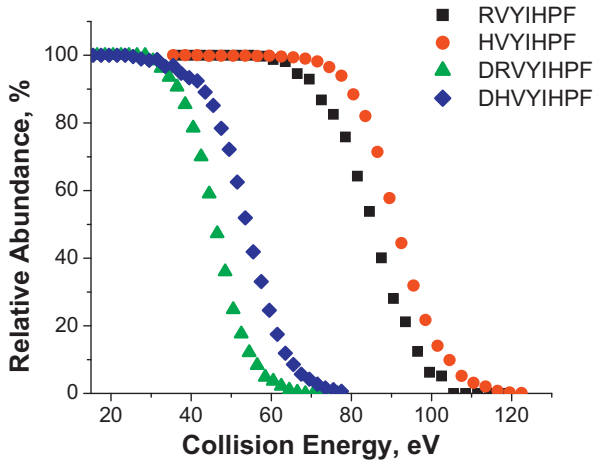

Fig. 3. Survival curves for $[M-H]^-$ precursor ions of RVYIHPF (filled square), HVYIHPF (open circles), DRVYIHPF (filled triangles), and DHVYIHPF (open diamonds).

($\Delta S^{\ddagger}$). Large kinetic shifts are associated with high reaction barriers and low activation entropies characteristic of tight transition states. For large molecules, the kinetic shift increases with decrease in reaction delay because even if the molecule is excited above the dissociation threshold it may not have enough time to fragment on a time scale of the experiment.

Comparison of protonated and deprotonated angiotensin analogs shows that although, as expected, higher $E_{50\%}$ values are observed at short delay times, the general trend in the relative stability of all species towards fragmentation is independent of the reaction time. Specifically, deprotonated DRVYIHPF, DHVYIHPF and RVYIHPF are less stable towards fragmentation than the corresponding protonated species, whereas the $[M-H]^-$ ion of HVYIHPF is the most stable species at all reaction delays. Interestingly, this is the only ion, for which fragmentation is dominated by backbone cleavages while other species undergo facile losses of small neutral molecules. Previous studies showed that addition of an acidic residue to a peptide sequence facilitates selective charge-remote fragmentation of protonated arginine-containing peptides that shifts the observed fragmentation towards lower collision energies [33,34]. Here we show that the presence of an acidic residue in the sequence has a substantially more pronounced destabilizing effect in the negative mode, which is reflected in very low values of $E_{50\%}$ obtained for deprotonated DRVYIHPF and DHVYIHPF. Finally we note that arginine-containing peptide anions (RVYIHPF and DRVYIHPF) are slightly less stable towards fragmentation than the corresponding species in which arginine is replaced with histidine (HVYIHPF and DHVYIHPF). In contrast, arginine has a strong stabilizing effect on singly protonated peptides. This effect is attributed to the high basicity of the arginine side chain that sequesters the ionizing proton [6,9]; this hinders proton-driven dissociation and often opens up alternative fragmentation pathways [35,36].

The stability of different ions towards fragmentation was further quantified using the RRKM-based modeling of SCs outlined earlier. Fig. 5 shows an example of the RRKM modeling for deprotonated

Table 2
Dissociation parameters for the total decomposition of deprotonated peptides examined in this study.

	RVYIHPF		HVYIHPF		DRVYIHPF		DHVYIHPF	
	$[M+H]^+$	$[M-H]^-$	$[M+H]^+$	$[M-H]^-$	$[M+H]^+$	$[M-H]^-$	$[M+H]^+$	$[M-H]^-$
E_0, eV	1.62	1.60	1.53	1.74	1.13	0.90	1.45	0.97
$\Delta S^{\ddagger}$, eu[a]	−3.9	−5.6	0.8	−5.5	−21.6	−24.5	−2.5	−23.7
A, s^{-1}	4×10^{12}	2×10^{12}	4×10^{13}	2×10^{12}	5×10^{8}	1×10^{8}	7×10^{12}	2×10^{8}
E (k = 1 s^{-1}), eV[b]	8.1	7.3	6.1	8.2	5.5	3.6	6.2	3.8

The estimated uncertainties are ±7% for threshold energies and ±3 eu for activation entropies.
[a] eu = entropy units = cal/(mol K); activation entropies and pre-exponential factors at 450 K.
[b] The internal energy of the ion necessary to obtain to the microcanonical rate constant of 1 s^{-1}.

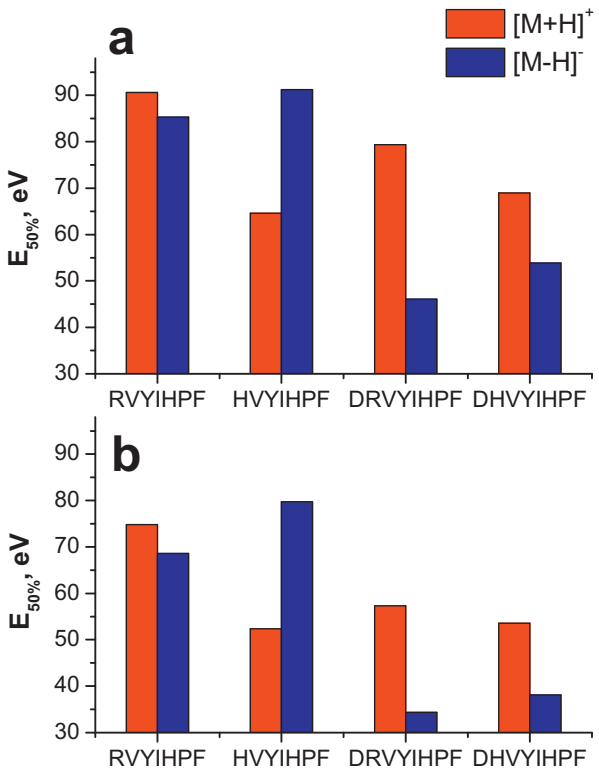

Fig. 4. Comparison of collision energies required to observe 50% fragmentation of the $[M+H]^+$ and $[M-H]^-$ ions of the four angiotensin analogs at two delay times of (a) 1 ms and (b) 1 s.

RVYIHPF, while the dissociation parameters for both $[M+H]^+$ and $[M-H]^-$ ions of all four peptides are summarized in Table 2. Similar threshold energies and activation entropies were obtained for $[M+H]^+$ and $[M-H]^-$ ions of RVYIHPF indicating that charge has no significant effect on the energetics and dynamics of dissociation of these species. It is interesting to note that fragmentation of both precursor ions is initiated by the loss of small neutral molecules: NH_3 and NHCNH for the $[M-H]^-$ ion and NH_3 for the $[M+H]^+$ ion [25,26]. Fig. 6 shows time- and collision energy resolved fragmentation efficiency curves (TFECs) obtained for these small neutral losses from $[M+H]^+$ and $[M-H]^-$ ions of RVYIHPF. Interestingly, only a small difference in TFECs is observed for the loss of NH_3 from

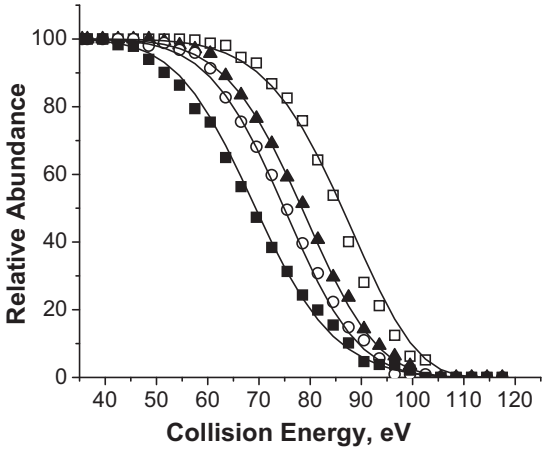

Fig. 5. RRKM modeling results fit to time resolved survival curves for deprotonated RVYIHPF. The modeling results are represented by solid lines while the points represent the experiment survival curves for reaction delays of 1 ms (open squares), 5 ms (filled triangles), 10 ms (open circles), and 1 s (filled squares).

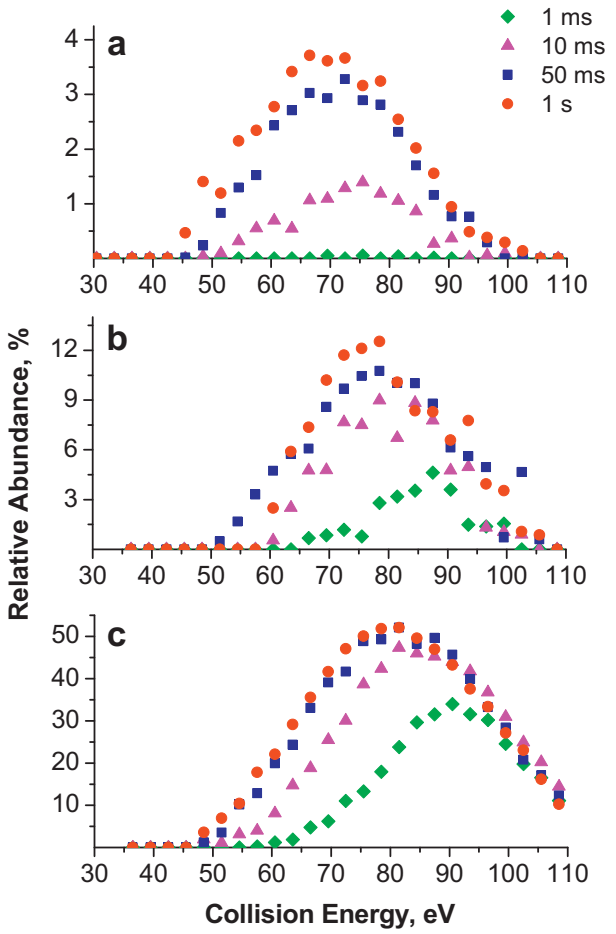

Fig. 6. TFECs for a) loss of NH_3 from $[M+H]^+$ ion, b) loss of NH_3 from $[M-H]^-$ ion, and c) loss of NHCNH from $[M-H]^-$ ion of RVYIHPF. The results are shown for delay times of 1 ms (diamonds), 10 ms (open triangles), 50 ms (squares), and 1 s (open circles).

the $[M+H]^+$ and $[M-H]^-$ ions. Similar energetics and kinetics of the NH_3 loss from the protonated and deprotonated RVYIHPF (Fig. 6a and b) indicate that loss of ammonia from this peptide most likely proceeds through a charge-remote pathway.

Loss of NHCNH (42 Da) from deprotonated RVYIHPF efficiently competes with the NH_3 loss (Fig. 6c). This fragmentation channel is commonly observed in MS/MS spectra of deprotonated peptides and peptides cationized on metals. Summerfield et al. suggested that this loss is produced through charge-remote fragmentation of the neutral arginine side chain [37]. Because of efficient protonation of the arginine side chain in $[M+H]^+$ ions this fragmentation pathway is not observed for protonated arginine-containing peptides such as RVYIHPF examined in this study. From the above discussion it follows that charge-remote dissociation pathways determine the relative stability of both positive and negative ions of RVYIHPF towards fragmentation.

Substitution of R with H blocks these charge-remote reaction channels and facilitates backbone fragmentation. This transition in the fragmentation behavior is associated with a ca. 0.14 eV increase in the dissociation threshold for the deprotonated molecule but has little effect on the activation entropy. Our results indicate that backbone fragmentation of the deprotonated molecules examined in this study is characterized by higher threshold energies than common side chain losses. Slightly smaller increase in the dissociation threshold of 0.07 eV is observed for DHVYIHPF as compared to DRVYIHPF. In contrast with the basic peptides, dissociation of $[M-H]^-$ ions of both DRVYIHPF and DHVYIHPF is characterized by a

large negative entropy effect indicating a very tight transition state for fragmentation. Entropy effects observed for deprotonated acidic peptides are comparable to activation entropies reported previously for selective fragmentation of protonated peptides [25,34] (see data for $[M+H]^+$ of DRVYIHPF in Table 2). It follows that similar to the protonated DRVYIHPF that undergoes selective fragmentation, loss of neutral molecules from deprotonated acidic peptides is associated with substantial rearrangement. Interestingly, much higher activation entropy was obtained for dissociation of the protonated DHVYIHPF. Low-energy fragmentation channels observed for this ion (data not shown) include loss of H_2O, the formation of the y_7 ion through selective cleavage at the aspartic acid, and the formation of the b_6 ion. The first two channels are kinetically hindered while the formation of the b_6 ion is a kinetically favored process. The presence of the fast primary dissociation pathway contributes to the observed increase in the activation entropy for protonated DHVYIHPF as compared to its deprotonated analog.

4. Conclusions

We presented a first quantitative experimental study of energy and entropy effects in gas-phase fragmentation of deprotonated angiotensin analogs as model systems for peptides containing acidic and basic residues. Collision-energy resolved SID experiments demonstrated that anions of acidic peptides undergo facile fragmentation at relatively low collision energies. The stability of the deprotonated peptides examined in this study inferred from the experimental values of $E_{50\%}$ increases in the order DRVYIHPF < DHVYIHPF ≪ RVYIHPF < HVYIHPF, which is quite different from the experimentally measured stability ladder observed in the positive mode: HVYIHPF < DHVYIHPF < DRVYIHPF < RVYIHPF. RRKM modeling of time- and collision-energy resolved survival curves provided quantitative information on the origin of the observed stability of deprotonated peptides. Specifically, we found that loss of H_2O, a dominant dissociation channel for acidic peptides, is characterized by low threshold energy and very tight transition state. The activation entropy for this pathway is comparable to the values obtained for selective cleavages in protonated systems while the energy barrier is significantly lower. As a result, deprotonated DRVYIHPF is much less stable towards fragmentation than its protonated analog. Substitution of R with a less basic H residue enhances non-selective fragmentation of the acidic peptide in the positive mode. Consistent with previous studies, entropically favorable non-selective fragmentation of DHVYIHPF is characterized by relatively high threshold energy.

In contrast with acidic peptides, decomposition of the positive and negative precursor ions of the most basic RVYIHPF peptide is characterized by similar energy and entropy effects. For this sequence, dissociation in both modes is initiated by small molecule losses. Interestingly, the charge state of the ion has only a minor effect on the kinetics of NH_3 loss indicating that this is most likely a charge-remote pathway. In contrast, charge state has a significant effect on the stability of HVYIHPF that lacks the basic arginine residue. For this system, protonation and deprotonation have opposite effects on the threshold energy for fragmentation and on the experimental value of $E_{50\%}$. Specifically, based on the experimental values of $E_{50\%}$, the deprotonated HVYIHPF that predominantly undergoes backbone cleavages is the most stable species examined in this study, while the protonated HVYIHPF is the least stable species. Our findings are important for developing a fundamental understanding of the factors that determine the quality of the structural information obtained from MS/MS experiments.

Acknowledgments

The research described in this paper was supported by the grant from the Chemical Sciences Division, Office of Basic Energy Sciences of the US Department of Energy (DOE). The research was performed at the W.R. Wiley Environmental Molecular Sciences Laboratory (EMSL), a national scientific user facility sponsored by the DOE's Office of Biological and Environmental Research and located at the Pacific Northwest National Laboratory (PNNL). PNNL is operated by Battelle for the US DOE. The authors thank Mr. Tao Song and Prof. Iven Chu for providing peptide samples.

References

[1] R. Aebersold, D.R. Goodlett, Chem. Rev. 101 (2001) 269–296.
[2] S.A. McLuckey, D.E. Goeringer, J. Mass Spectrom. 32 (1997) 461–474.
[3] J. Laskin, J.H. Futrell, Mass Spectrom. Rev. 22 (2003) 158–181.
[4] J.B. Fenn, M. Mann, C.K. Meng, S.F. Wong, C.M. Whitehouse, Science 246 (1989) 64–71.
[5] M. Karas, D. Bachmann, U. Bahr, F. Hillenkamp, Int. J. Mass Spectrom. Ion Process. 78 (1987) 53–68.
[6] A.R. Dongre, J.L. Jones, A. Somogyi, V.H. Wysocki, J. Am. Chem. Soc. 118 (1996) 8365–8374.
[7] M.J. Polce, D. Ren, C. Wesdemiotis, J. Mass Spectrom. 35 (2000) 1391–1398.
[8] A. Schlosser, W.D. Lehmann, J. Mass Spectrom. 35 (2000) 1382–1390.
[9] V.H. Wysocki, G. Tsaprailis, L.L. Smith, L.A. Breci, J. Mass Spectrom. 35 (2000) 1399–1406.
[10] B. Paizs, S. Suhai, Mass Spectrom. Rev. 24 (2005) 508–548.
[11] J. Laskin, Energy and entropy effects in the gas phase dissociation of peptides and proteins, in: J. Laskin, C. Lifshitz (Eds.), Principles of Mass Spectrometry Applied to Biomolecules, John Wiley & Sons, Inc., Hoboken, NJ, 2006.
[12] V.H. Wysocki, G. Cheng, Q. Zhang, K.A. Herrmann, R.L. Beardsley, A.E. Hilderbrand, Peptide fragmentation overview, in: J. Laskin, C. Lifshitz (Eds.), Principles of Mass Spectrometry Applied to Biomolecules, John Wiley & Sons, Inc., Hoboken, NJ, 2006.
[13] C.K. Barlow, R.A.J. O'Hair, J. Mass Spectrom. 43 (2008) 1301–1319.
[14] J.H. Bowie, C.S. Brinkworth, S. Dua, Mass Spectrom. Rev. 21 (2002) 87–107.
[15] R.J. Waugh, J.H. Bowie, R.N. Hayes, Int. J. Mass Spectrom. Ion Process. 107 (1991) 333–347.
[16] E.M. Marzluff, S. Campbell, M.T. Rodgers, J.L. Beauchamp, J. Am. Chem. Soc. 116 (1994) 7787–7796.
[17] C.S. Brinkworth, S. Dua, A.M. McAnoy, J.H. Bowie, Rapid Commun. Mass Spectrom. 15 (2001) 1965–1973.
[18] A.G. Harrison, A.B. Young, Int. J. Mass Spectrom. 255 (2006) 111–122.
[19] J. Jai-nhuknan, C.J. Cassady, J. Am. Soc. Mass. Spectrom. 9 (1998) 540–544.
[20] N.P. Ewing, C.J. Cassady, J. Am. Soc. Mass. Spectrom. 12 (2001) 105–116.
[21] N.L. Clipston, J. Jai-nhuknan, C.J. Cassady, Int. J. Mass spectrom. 222 (2003) 363–381.
[22] D. Pu, N.L. Clipston, C.J. Cassady, J. Mass Spectrom. 45 (2010) 297–305.
[23] N. Bache, K.D. Rand, P. Roepstorff, M. Ploug, T.J.D. Jorgensen, J. Am. Soc. Mass. Spectrom. 19 (2008) 1719–1725.
[24] J. Laskin, E.V. Denisov, A.K. Shukla, S.E. Barlow, J.H. Futrell, Anal. Chem. 74 (2002) 3255–3261.
[25] J. Laskin, T.H. Bailey, J.H. Futrell, Int. J. Mass spectrom. 234 (2004) 89–99.
[26] J. Laskin, T.H. Bailey, J.H. Futrell, Int. J. Mass spectrom. 249 (2006) 462–472.
[27] Z. Yang, E.R. Vorpagel, J. Laskin, J. Am. Chem. Soc. 130 (2008) 13013–13022.
[28] J. Laskin, Z. Yang, I.K. Chu, J. Am. Chem. Soc. 130 (2008) 3218–3230.
[29] J. Laskin, M. Byrd, J. Futrell, Int. J. Mass spectrom. 195 (2000) 285–302.
[30] J. Laskin, J. Futrell, J. Phys. Chem. A 104 (2000) 5484–5494.
[31] A.G. Harrison, J. Am. Soc. Mass. Spectrom. 12 (2001) 1–13.
[32] C. Lifshitz, Eur. J. Mass Spectrom. 8 (2002) 85–98.
[33] G. Tsaprailis, A. Somogyi, E.N. Nikolaev, V.H. Wysocki, Int. J. Mass spectrom. 195 (2000) 467–479.
[34] T.H. Bailey, J. Laskin, J.H. Futrell, Int. J. Mass spectrom. 222 (2003) 313–327.
[35] B.J. Bythell, S. Suhai, A. Somogyi, B. Paizs, J. Am. Chem. Soc. 131 (2009) 14057–14065.
[36] J. Laskin, Z. Yang, T. Song, C. Lam, I.K. Chu, J. Am. Chem. Soc. 132 (2010) 16006–16016.
[37] S.G. Summerfield, V.C.M. Dale, D.D. Despeyroux, K.R. Jennings, Eur. Mass Spectrom. 1 (1995) 183–194.